Archaeological studies at Dholavira using GPR

Silky Agrawal[1], Mantu Majumder[1], Ravindra Singh Bisht[2] and Amit Prashant[1,*]

[1]Civil Engineering, Indian Institute of Technology Gandhinagar, Palaj, Gandhinagar 382 355, India
[2]9/19, Sector III, Rajendra Nagar, Sahibabad, Gaziabad 201 005, India

A new area at an existing archaeological site of Harappan civilization at Dholavira, Gujarat, India has been studied using ground penetrating radar (GPR). An area of 12,276 m^2 was surveyed using 200 MHz antenna at grid spacing of 2–3 m. The soil strata was found to extend mainly up to 3.5–4 m. The survey was conducted during the dry season to collect good signals. Post-processing was carried out to map the bedrock as well as archaeological features. A number of linear features were observed from the 3D image of the subsurface created from the acquired GPR profiles. Unlike residential structures, the large dimensions of these features indicate the likely existence of a series of water structures that may have partly collapsed due to floods at some point. There were some areas full of rubble next to the damaged walls that appeared to be orthogonal to the direction of possible flood from Manhar River.

Keywords: Archaeology, electromagnetic waves, ground penetrating radar, water reservoirs.

GROUND penetrating radar (GPR) is a tool capable of non-destructively imaging the subsurface. It is based on electromagnetic (EM) technique and provides high-resolution subsurface profiles which help in effectively mapping the underground features. Since the operation of GPR includes transmission, propagation and reflection of high frequency EM waves, the performance depends on the electrical properties of the host as well as the target materials.

Moreover, there is a trade-off between depth of penetration and the capability of resolving target objects depending upon the centre frequency of the antenna used and electrical conductivity of the host material. Therefore, high-frequency antenna are capable of resolving small objects at shallow subsurface, whereas low-frequency antenna can resolve larger objects at greater depths. GPR can be effectively applied to detect metallic as well as non-metallic anomalies in various domains such as soil, water, ice, concrete, etc.[1–6].

GPR is capable of 3D imaging of the subsurface, which extends its application in the study of buried archaeological features. Conyers[7] explained various field parameters of GPR for its archaeological application with basic processing strategy. He also identified historical graves using GPR on the basis of reflections from the vertical shafts and partially damaged coffins[8]. It also explained how reflections from the grave were different from those due to the presence of tree roots and other buried remains. Muztaza and Saad[9] used GPR 3D imaging to map the earthen furnace and other structures of archaeological interest in Jeniang Kedah, Malaysia. Kaneda *et al.*[10] utilized GPR survey to promote archaeological prospection in Japan. The sites comprised mainly of wooden structures that left only traces after decomposition. Therefore, with GPR data it was difficult to exactly interpret the features; however, it was possible to find the location of the area for excavation up to a certain extent.

Various studies propose different ways of data collection during GPR survey to achieve improved resolution of 3D subsurface images[11–13]. Researchers have also studied different locations for buried archaeological artefacts, hearths, graves and other such features using various approaches for 3D visualization, such as conventional time-slice technique and iso-amplitude technique[14–18]. The raw GPR data collected from the survey first need to be processed appropriately for interpretation. Various processing strategies have been proposed for adequate processing of GPR data[19–22], with examples of GPR profiles presenting reflection patterns of different archaeological features which are difficult to interpret[7,19–25]. It can be challenging sometimes to interpret different archaeological features from reflection patterns in the GPR profile. For convenience of possible interpretations, typical features and their reflections have been summarized in Appendix 1, after a review of several sources of information.

The present study investigates a new area at an existing archaeological site of Harappan civilization at Dholavira, Gujarat, western India, to explore the possibility of buried structures using GPR survey. Besides this, the rock profile of the area is also analysed. Dholavira is one of the most prominent archaeological sites situated at Khadirbet in Bhachau taluka, Kutch district, Gujarat. The site is surrounded by salt pans of the Great Rann of Kutch and consists of the ruins of an ancient Indus Valley Civilization. The city existed from about 3000 to 1700 BCE, in an area of around 100 ha with 48 ha under fortification. The whole city space of Harappan civilization in Dholavira is principally divided into three components consisting of a citadel, a middle town and a lower town as

*For correspondence. (e-mail: ap@iitgn.ac.in)

residential area. It also includes two stadia, an annexe and a series of reservoirs, running around the whole area. The Harappan city at Dholavira is known for its elegant planning, historic structures, artful architecture, fascinating water-harvesting system and a variety in funerary architecture[26].

There were several unexplored areas inside the city space, such as to the east of the East Reservoir, between the East Reservoir and the South Reservoir, in the northeast of the middle town, in the northeast of the lower town, etc. which may contain ruins of the ancient city. However, according to Bisht[26], the area towards east of the East Reservoir is expected to contain ruins of a series of possible water-harvesting structures similar to the East Reservoir excavated earlier. Therefore, the present study was conducted to map the buried archaeological features non-destructively using GPR survey for efficient exploration of the unexcavated area situated to the east of the East Reservoir.

The survey was conducted at two nearby sites covering the total area of 12,276 m^2. The site was laid close to the northern bank of the Manhar River and extended towards northeast from the southeast corner of the East Reservoir.

Layout of the area and methodology of GPR survey

The area situated to the east of the East Reservoir and south of the lower town was chosen for the study using GPR (Figure 1). The area was demarcated into rectangles up to maximum possible accessibility in north–south (NS) and east–west (EW) directions for efficient survey, as the excavated structures of Harappa civilization were found to be aligned in standard NS direction. Table 1 shows the dimensions of each rectangular block. The East Reservoir is marked on the plan for reference; however, the northwest corner of block A1 is 24 m away with bearing of 132°30′ from the northeast corner of the East Reservoir.

Data acquisition in field

The area was surveyed using GSSI SIR-3000 GPR system in February and March 2015. Figure 1 shows the marked areas for the survey. Considering the size of the area and the expected sizes of archaeological features, the survey was carried out initially at grid spacing of 3 m in both NS and EW directions. Since the depth of archaeological features in the area was largely unknown at the initial stage, the survey was conducted using antennas of centre frequency 400 and 200 MHz. Using 400 MHz antenna, the data were collected in distance mode with 50 scans per unit metre, time window of 50 ns, and transmission rate of 100 kHz and with the antenna in mono-static mode. While using 200 MHz frequency antenna, data were collected in a similar fashion with 35 scans per unit metre, time window of 160 ns to cover greater depth, and transmission rate of 100 kHz. Subsequently, a few potential zones containing the archaeological features were identified on the basis of the first survey and the survey was again conducted in these zones with finer resolution grid at transect spacing of 1–2 m in both directions. The second survey helped confirm the consistency of the reflections observed in the profiles of the first survey.

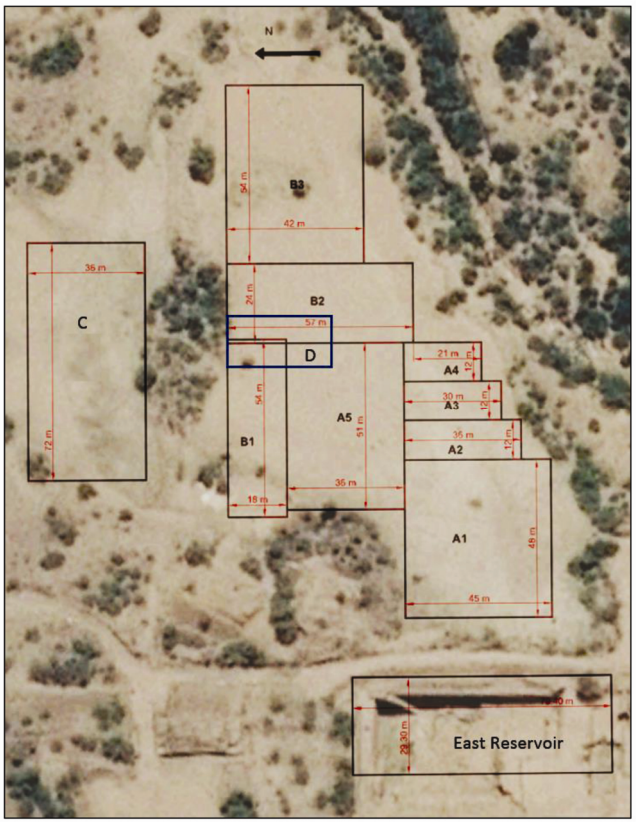

Figure 1. Layout of the studied area at Dholavira, Gujarat, east of the East Reservoir.

Table 1. Dimensions of rectangular blocks in the studied area

Area code	North–south dimension (m)	East–west dimension (m)
A1	45	48
A2	36	12
A3	30	12
A4	24	12
A5	36	51
B1	18	54
B2	57	24
B3	42	54
C	36	72
D	36	18

Data processing

The raw data acquired in the field were appropriately processed using the commercial software RADAN (GSSI), to generate data interpretable for archaeological features. Primarily, time-zero correction was applied to the whole dataset to ensure zero time at zero depth from the ground surface, followed by background removal of unwanted banding noise. Further, band-pass filter of 100 –500 MHz for 400 MHz antenna and 50–250 MHz for 200 MHz antenna was applied to filter out unwanted low- and high-frequency contents from the profile data followed by application of range gain using exponential function defined at 16 points along the scan to amplify the deeper weak signals. Lastly, the velocity of EM wave was estimated as 0.12 m/ns based on Kirchhoff's migration analysis of data recorded on GPR 2D profiles using RADAN software. The depth of different targets was estimated using eq. (1)

$$d = \frac{vt}{2}, \tag{1}$$

where d is the depth of the target, v the EM wave velocity in the medium and t is the two-way travel time of the reflected EM wave. Hence, two sets of processed 2D profiles were obtained for 200 and 400 MHz antenna respectively. However, 400 MHz antenna data provided hyperbolic reflections in a rather shallow region and did not show any specific pattern, which was likely to be from the modern fill soil and hence discarded. Therefore, processed data of 200 MHz antenna have been mainly utilized for creating 3D view of subsurface and further interpretations.

Rock profile analysis of the area

Processed 2D profiles were observed to find the bedrock level at the studied site. However, bedrock was not clearly visible in all the profiles and therefore processed further by applying band-pass filters and deconvolution on the initially processed signals. Subsequently, the bedrock depth was identified at various points in the studied area, which showed that the bedrock level varied from 3.5 to 4.2 m. There were only a couple of locations where it was around 2 m in small areas. It was also observed that the bedrock had gentle slope of 0.9% towards west between areas A1 and B2; however, the ground had a slope of 0.7% towards east, and hence the bedrock was found to be almost flat. At one location shallow interruptions were also observed at a depth of 1.0–1.5 m below bedrock level, possibly due to natural change in the bedrock level, since this area is in the vicinity of the Manhar River. Another possibility could be man-made depression in the bedrock for laying the foundation for dams or bunds.

Identification of buried features from processed GPR data

The 3D view of the subsurface was obtained independently for each rectangular block. However, the possible archaeological features were observed in only some of the rectangular blocks and details of only those sections have been presented here.

Observations in area A

Figure 2 *a* shows 3D subsurface view at depth slices of 0.75, 1.5, 2.25 and 3 m in area A1. Interpretations based on these depth slices provide traces of the existence of some linear features. Two linear features have been identified, which are about 7 m apart with 33–36 m length along the EW direction. These features are faintly visible in 1.5 m deep slice. The reflections are stronger at deeper level and become clearly visible in 3 m deep slice. Similar dual linear features about 8–10 m apart are observed along the whole length in the NS direction at a distance of 33–36 m towards west. Figure 2 *b* shows the depth slices at 0.75, 1.5, 2.25 and 3 m for a part of area A5. This area also shows dual linear features along the NS direction in continuation of the similar linear feature in area A1. However, in this area the features are visible at a 2.25 m depth slice unlike at 1.5 m depth slice in area A1, and become more prominent in 3 m depth slice. Hence, the dual linear features of areas A1 and A5 are possibly from the same structure, but the upper part of the wall may have been partially damaged or demolished earlier. The scattered reflections in the profile also indicate the possibility of damaged or undulating top surface of the structure.

Further, reflection patterns in all the 2D profiles were analysed to make additional interpretations related to the type of features. For example, Figure 3 *a* shows part of one sectional profile containing the feature along the NS direction, across the linear feature at a distance of 9 m from the origin. The two prominent reflections, 1.5 m deep extending up to around 5 m, are marked in the figure. These features were difficult to interpret directly; however, the reflections resembled the expected reflection pattern of walls as discussed in Conyers[24]. Hence, these linear features can be interpreted as two parallel walls around 8 m apart. Similarly, the sectional 2D profiles have been observed along the EW direction across the expected wall features perpendicular to the previous one. The section views confirmed the existence of dual walls.

In addition to the collected data, three extra profiles were collected along the footpath between the East Reservoir and area A1 to check the existence of ruins of any connecting structure, as the area was not accessible enough to collect the data in grid. The profiles indicated

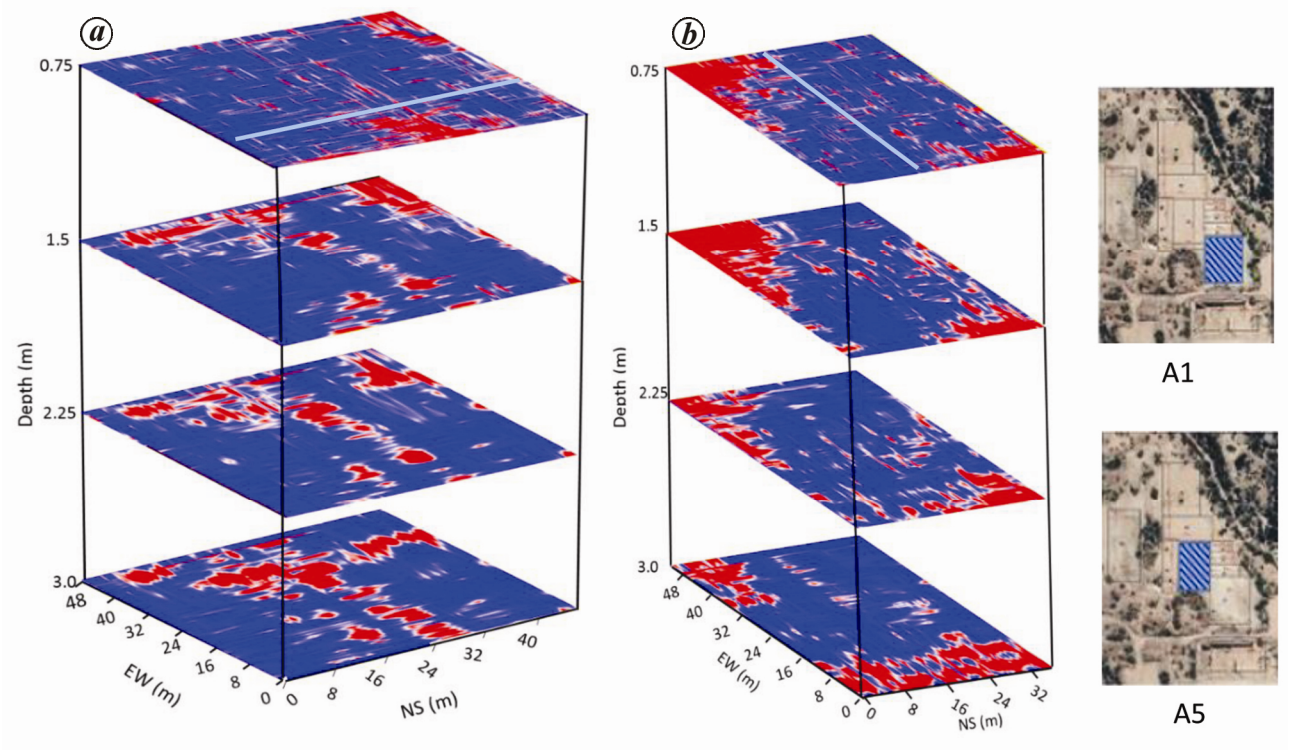

Figure 2. Depth slices of GPR data in (***a***) area A1 and (***b***) area A5.

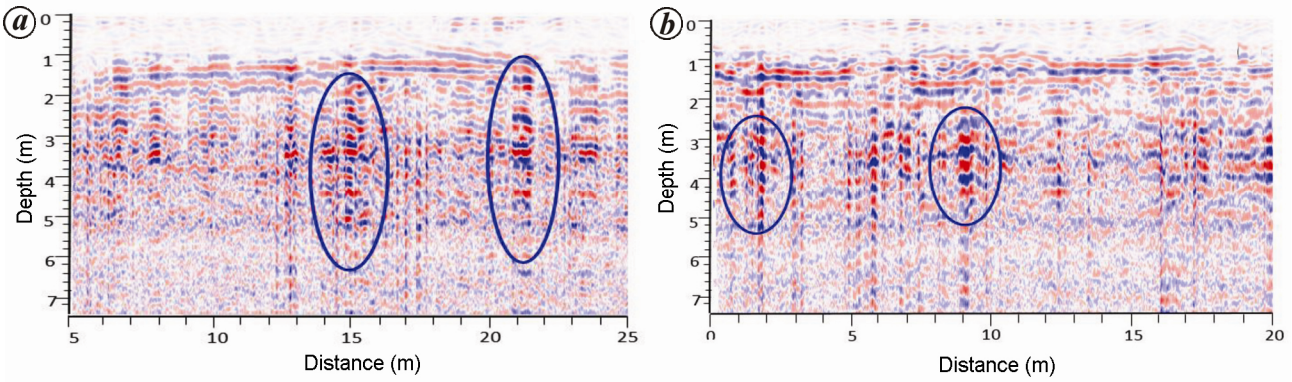

Figure 3. Select GPR profiles showing marked signatures across linear features along (***a***) NS direction in area A1 and (***b***) EW direction in area A5.

the existence of similar wall type of features as in area A1 and showed the continuity towards the East Reservoir.

The sectional profile given in Figure 3 *b* along the EW direction of area A5 indicates that the wall type of feature identified in area A1 continues in area A5 as well. Similarly, a number of sectional views have been reviewed for this area. From this a NS linear feature is found towards the northeast of A5, although the 3D subsurface view shown in Figure 2 *b* does not clearly identify the same. Furthermore, high-amplitude reflections were observed at the northwest and southeast corners of area A5. The complex linear and hyperbolic signatures in 2D GPR profiles across these high reflections indicate the existence of boulder or rubble deposit rather than any constructed feature.

The GPR profiles of areas A2, A3 and A4 have been also analysed in a similar fashion and some minor linear features were observed. The analysis suggests the existence of an inclined wall extending from A2 to A3. Similarly, one more linear feature is likely to be present along the EW direction extending from A2 to A4. In Figure 4, the interpreted features of area A have been marked at the depth slice of 3 m.

Observations in area B

The 3D subsurface views of rectangular patches B1, B2 and B3 of area B were analysed at different depth slices, similar to area A. Intense scattered reflections were

observed with some linear features in this area. The 2D sectional profiles were analysed across these reflections. The reflection pattern in area B1 suggests the existence of one wall towards the eastern part of area B1, which is aligned with the wall identified in area A5 and surrounded by rubble deposit. Similarly, the sectional profiles of area B2 indicate the existence of a NS wall in the western part of area, parallel to the wall identified in areas A5 and B1, followed by rubble deposits towards south of the area. The 2D sectional profile of area B3 shows intense reflections suggesting the existence of rubble deposit slanting in the south direction (Figure 5 *a*). The rubble deposit is found to continue from area B2 extending towards the northeast corner of the area. Two parallel NS wall features were also observed, a part of it towards north exposed as a mound to the ground surface. Figure 5 *b* shows the 3D subsurface view of area B with marked interpretations. As the linear features were observed in area A5 continuing in B1 and parallel wall in area B2, a finer resolution survey with 1 m transect spacing was conducted in a patch of 36 m × 18 m (area D in Figure 1), to confirm the existence of the parallel walls. The existence of a closed rectangular structure at a depth of around 1.5 m could be interpreted on the basis of depth slices of area D. Moreover, the sectional profiles of area D along the EW direction suggest the presence of two linear features in the NS direction. Although it could be a closed rectangular feature, there is no clear signature of EW features in the profiles. It is possible that the EW features might have got washed away by a possible huge flood-water thrust.

Observations in area C

The depth slices of area C are shown in Figure 6 *a*, which suggests the existence of a NS linear feature along the south edge of the area and EW linear features along the west edge as well as at a distance of 39 m from it. Further, the 2D sectional profiles along the NS and EW directions (marked in Figure 6 *a*) across these linear features also show the existence of similar wall-like features at a depth of about 1 m (Figure 6 *b* and *c* respectively).

Weak signal analysis

The 3D subsurface view obtained in the conventional processing suggested possible existence of linear features; however, in some cases it was difficult to clearly confirm the exact feature reflections in the conventionally processed sectional 2D profiles. Therefore, the whole GPR data collected in the area were further processed using the time–frequency (TF) method proposed by Agrawal *et al.*[27] for the existence of any other feature which was not visible in conventionally processed time-domain GPR profiles. These sectional profiles obtained from TF processing enhanced the feature reflections by removing the extra ambiguous reflections in the profile and thus, provided confidence in the interpreted features. Figure 7 shows the improved profiles using the TF

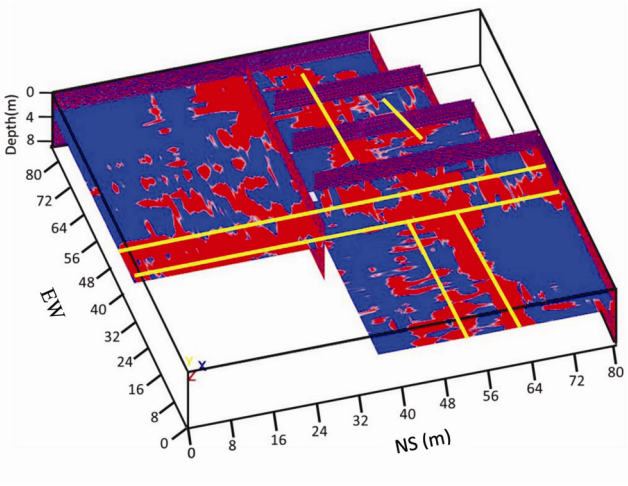

Figure 4. Depth slice of GPR data in area A with marked interpretations.

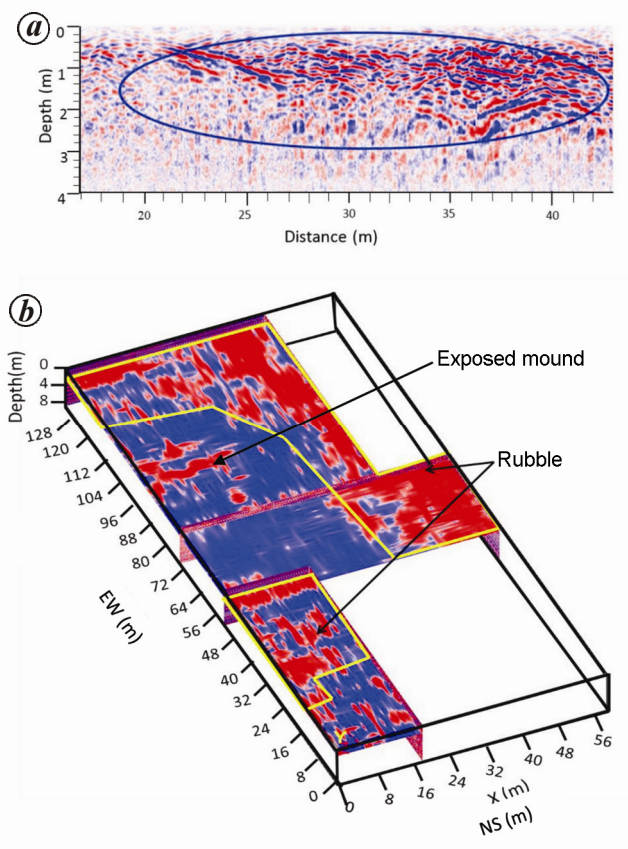

Figure 5. GPR data of area B. ***a***, A sectional profile in NS direction showing complex signatures. ***b***, Depth slice of the area with marked interpretations.

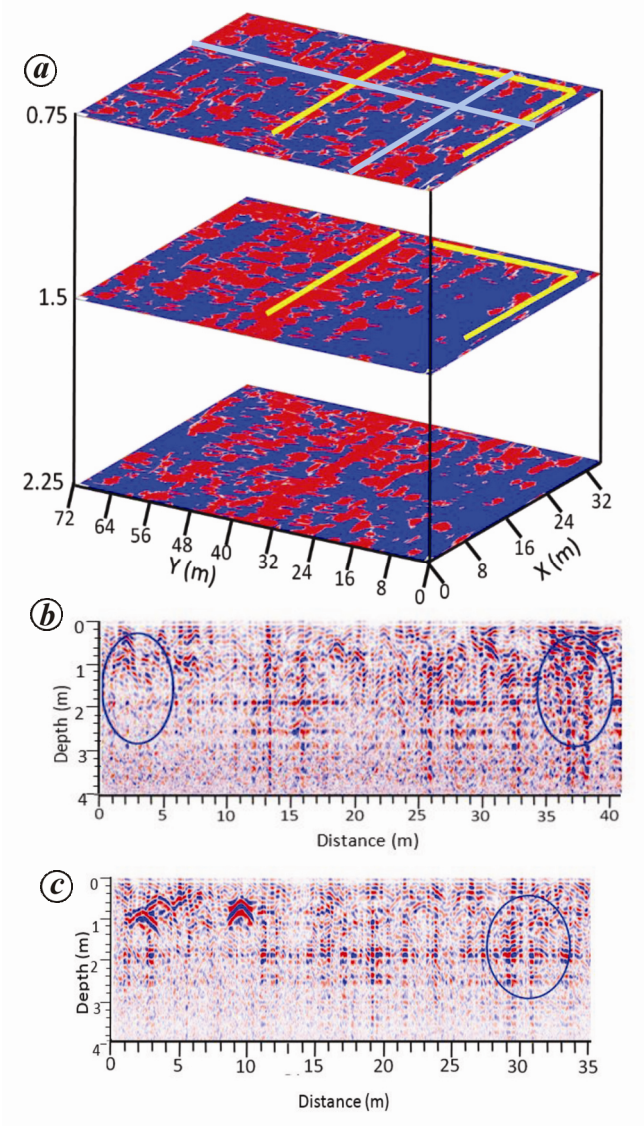

Figure 6. GPR data of area C. ***a***, Depth slices of the area with marked interpretations. ***b***, ***c***, Select sectional profiles along EW (***b***) and NS (***c***).

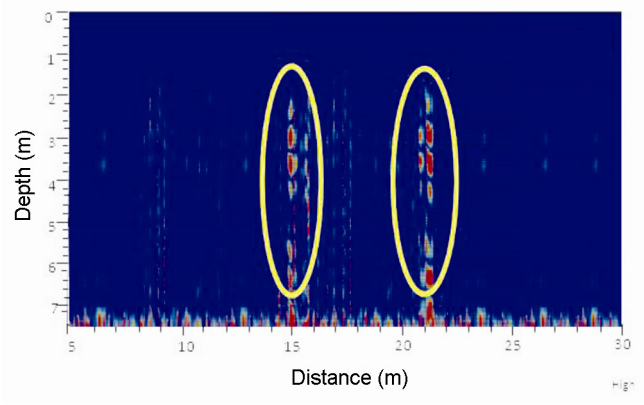

Figure 7. Improved GPR profile along NS direction of area A1 using time–frequency analysis.

method corresponding to the conventionally processed profiles of Figure 3 *a*. The two localized signatures in the profile represent reflections from the wall-like features that were difficult to locate exactly in the conventionally processed profile. Similar processing of GPR data from other locations did not show any new features.

Archaeological interpretations of the identified features

The objective of archaeological interpretation is to correlate the observed features from GPR study with the possible archaeological features based on the other exposed features existing in the nearby areas and the geographical conditions of the site. The major features identified in the studied area are shown in Figure 8 to provide the spatial location of these identified features with respect to the exposed structures. In this figure, F1 represents the rectangular feature of C-shape in area C open in the north, F2 the two linear features between areas A and B, F3 the rubble spread in area B, F4 the two pairs of linear wall-like structures, one running in the NS direction with length of about 80 m and the other along EW direction of length about 33 m, and F5 represents the dual non-parallel linear features in area A. The region to the south of area A1 was not surveyed due to inaccessibility of the site for GPR survey; therefore, existence of F1 beyond area A was not checked. The surveyed area to the east of F1 shows that this feature terminates at the NS wall. Further, there is no feature found in area B for continuity of the same towards north.

The studied area is surrounded by the Manhar River flowing from east to west. Geographical details of the area suggest that the overall site is gently sloping towards west, thus during floods the overflow water can only flow towards the surveyed area which may have caused damage in some of the structures. The presence of the grand East Reservoir and a series of reservoirs excavated earlier suggests that the Harappans had a good water-harvesting system. Therefore, the studied area is expected to have similar kinds of reservoirs, bunds, check dams, channels, drains and water tanks. Moreover, the observed features in the GPR data are of large dimension and resemble the reservoir-type of structures, unlike the residential structures of smaller size. All the features of areas A and B are found to be at depth of 1.5 m, whereas in area C they are at 1 m depth from the ground surface. Since there is ground-level difference of about 0.75 m between these two areas, the identified features in both the locations are approximately at the same reference level. Thus, the possibilities of water-harvesting-type structures based on the observed features were further explored (Figure 9).

For example, F1 in area C possibly can be part of a shallow water-storage tank used to collect surface run-off

water from the lower town of the city space to its north. The feature F2 in areas A and B can be a closed structure forming a small reservoir for water harvesting. However, no distinct boundary wall was observed along the EW direction connecting the NS linear features. It is perceived that the Harappans may have built a small dam on the Manhar River to divert its water towards the series of reservoirs around the citadel. It is possible that the water diverted from the dam during a flash flood may have damaged the EW wall of the structure of F2 and left only the NS wall intact. The rubble deposit observed in area B relates to the ruins of the possibly collapsed EW wall. Further, it is possible that these two features (F1 and F2) were interconnected forming a series of reservoirs. However, existence of the connecting channel was not confirmed in this study due to inaccessibility of the region between areas B and C.

Another probable interpretation for the dual linear feature of F2 may be that it is one among a series of three possible bunds marked as D1–D3 in Figure 9. The mound exposed to the ground surface in the east of F2 (bund D3) can be the second bund (marked as D2) and the third bund D1 appears to have collapsed at some point of time and resulted into a local spread of rubble of feature F3. It is possible that the Harappans raised several bunds or dams towards the east of the area to obstruct the flow of water from the Manhan River and protect important reservoir structures from the flood-water thrust. The two reflections separated by the scattered reflections in GPR sectional profiles endorse that the Harappans had constructed these types of bunds by raising two separate walls and filling stone rubble or mud brick between them.

The feature F4 can be hypothesized as part of a pair of small shallow reservoirs, assuming possible existence of similar features parallel to the NS and EW walls. Since the overall site slope is towards the west, water from the channel near the fortification wall is expected to have flown from east to west towards the citadel. High flow of water during floods in the Manhar River may have been seen as a potential threat to the grand East Reservoir. The Harappans may have probably constructed two small reservoirs just before the East Reservoir to reduce the impact of initial high velocity flow, so that the large reservoir is partially filled through connecting channels before direct flow of water reaches it. The bedrock level at location F4 shows no sudden change from the surrounding areas; hence, the reservoir depth is likely to be shallow. This information also endorses the hypothesis that these two reservoirs were not merely used for water storage, but to protect the grand East Reservoir in the

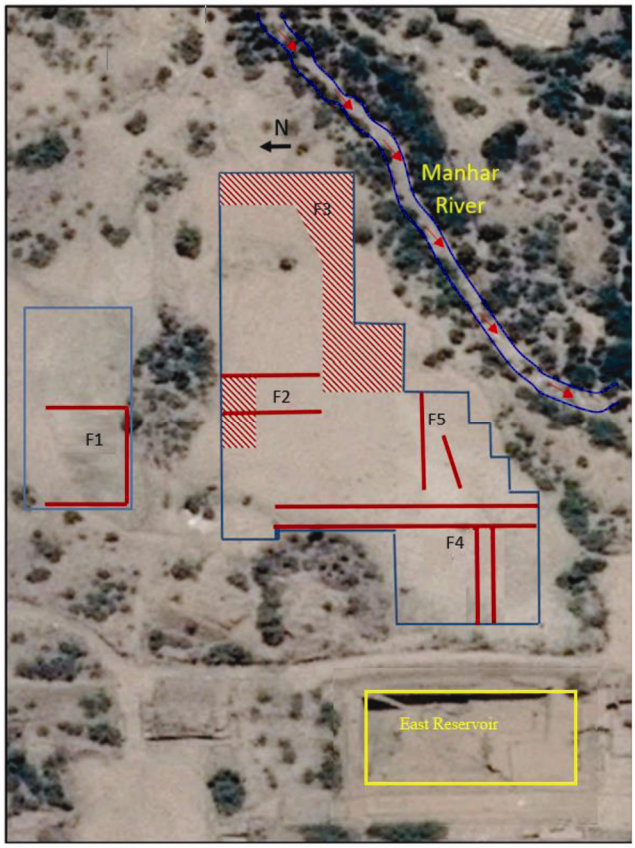

Figure 8. Observed features from the collected GPR data in the surveyed area at Dholavira.

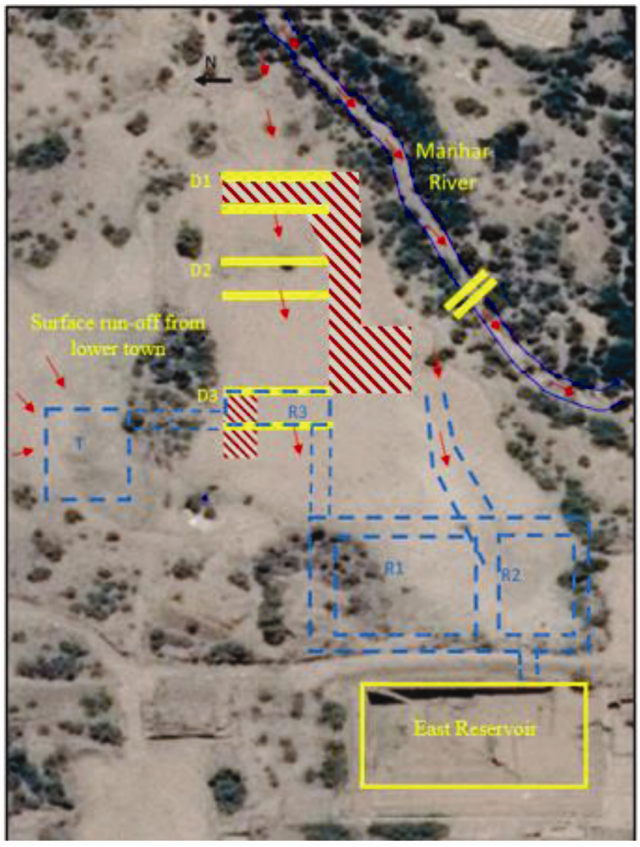

Figure 9. Archaeological interpretations based on the observed features from GPR study in the east of the East Reservoir at Dholavira.

Appendix 1. Signatures and limitations of common features using GPR

Item	Signature	Remarks
Wall[12,24,28]	Hyperbolic, half hyperbolic or multiple reflections (from interfaces) in sectional profile.	Weak reflection if made of homogeneous clay (low dielectric contrast).
Floors[24]	Linear reflection when intact. Plastered, burned and compacted earth or clay floors produce high-amplitude reflections.	Often distorted or jumbled reflections due to variable EM wave velocity or interfering hyperbolic reflections.
Voids[5,29,30]	Large negative peak at the soil–air interface. Often multiple reflections due to resonance scattering of waves.	Large positive peak for water-filled voids.
Canals[24]	Bow-tie reflections for narrow canals with steep banks. Multiple reflections from bowl-shaped canal beds.	Faint reflection from canal edges. Indistinct reflections with the same material deposit of sediments at the base.
Metals[31]	Multiple reflections of constant period; repeating or 'echoing' bands in sectional profile.	Corroded iron objects produce weak reflections.
Wooden targets[24,32]	Strong reflections for moistened wood in relatively dry medium.	Weak reflection for dry wood in dry medium; no distinct reflection when wood is decomposed.
Pipes[5,33]	Clear hyperbolic reflections; metal pipes with first positive peak; hollow concrete and plastic pipes with first negative peak.	Sometimes multiple reflections in non-metallic pipe as well. Indistinct reflection for similar material inside and outside the pipe.
Tree roots[34,35]	Generally strong hyperbolic reflections.	No specific reflection from destroyed tree roots or roots in high moisture soil.
Stones[24,29]	Strong hyperbolic reflection.	Weak reflection for stones with similar electrical properties as the surrounding soil.
Water table[36]	Continuous high-amplitude reflections.	Sometimes it may be wrongly interpreted as change of strata.

west and also act as supporting structures in the complete hydraulic system. The Harappans had applied excellent hydraulic engineering technique in laying out a series of reservoirs as interpreted from the already exposed areas, with some reservoirs used for sedimentation and siltation, and some for storing water. Therefore, the small reservoirs probably also served as water purifying systems before water reached the East Reservoir as a storage tank.

The feature F5 can be interpreted as a channel carrying water from an ancient dam exposed on the Manhar River to the East Reservoir. These features appear to form a channel with increasing cross-sectional area towards the west, in the direction of flow of water, resulting in decreased speed of flowing water and hence preventing potential damage to the water-storage structures.

The interpretations from GPR data were made logically on the basis of available information about the geographical features of the area, details of the structures exposed or those excavated by the Harappans and construction styles of the Harappan civilization from studies related to Dholavira. However, the existence of these structures can only be confirmed by careful archaeological excavations.

Conclusion

The GPR survey data of 12,776 m^2 area from the Harappan site at Dholavira have been analysed to map the possible archaeological features to the east of the grand East Reservoir. Two T-shaped parallel walls were found at an average spacing of 7–8 m along the NS and EW directions in the western part of the area. To the east of this T-shape feature, there was a set of linear features aligned in the NS along with a spread of rubble localized to the south. Further, in another area towards north (south of lower town), a C-shaped feature was found that had an opening in the north. From GPR data analysis, rock profile of the area was found to be almost flat. The archaeological interpretation of these features suggested the existence of a set of small and shallow reservoirs possibly connected with other. Part of these reservoirs, especially the wall aligned in the EW direction, may have collapsed during a flash flood at some point of time and deposited as rubble around it. Some of the features in the east may be alternatively interpreted as check dams, which may have collapsed due to flash flood from Manhar River. The interpreted archaeological structures on the basis of the identified features in the GPR data have been marked on the area map to provide spatial location with respect to the existing structures.

1. Maser, K. R., Condition assessment of transportation infrastructure using ground-penetrating radar. *J. Infrastruct. Syst.*, 1996, **2**, 94–101.
2. Maierhofer, C., Nondestructive evaluation of concrete infrastructure with ground penetrating radar. *J. Mater. Civ. Eng.*, 2003, **15**, 287–297.
3. Tallini, M., Giamberardino, A., Ranalli, D. and Scozzafava, M., GPR survey for investigation in building foundations. In

Proceedings of the Tenth International Conference on Ground Penetrating Radar, 2004, vol. 1, pp. 395–397.
4. Chen, D. H. and Wimsatt, A., Inspection and condition assessment using ground penetrating radar. *J. Geotech. Geoenviron. Eng.*, 2009, **136**, 207–214.
5. Hebsur, A., Muniappan, N., Rao, E. P. and Venkatachalam, G., A methodology for detecting buried solids in second-use sites using GPR. In Proceedings of the Indian Geotechnical Conference, Geotrendz, IIT Bombay, 2010.
6. Prasad, P. and Boopalan, A. J., Ground penetrating radar a tool to map the seismically induced fault and fracture in the coastal cliff of East Coast of Port Blair, Andaman. *Arpn. J. Earth Sci.*, 2013.
7. Conyers, L. B., *Ground-Penetrating Radar for Archaeology*, AltaMira Press, 2013.
8. Conyers, L. B., Innovative ground-penetrating radar methods for archaeological mapping. *Archaeol. Prospect.*, 2006, **13**, 139–141.
9. Muztaza, M. M., Saidin, M. M., Azwin, I. N. and Saad, R., Archaeological structure detection using 3D GPR survey in Jeniang, Kedah, Malaysia. In International Conference on Geological and Environmental Sciences, South Korea, 2012, vol. 36, pp. 49–53.
10. Kaneda, A., Nishimura, Y. and Nishiguchi, K., To find post holes: application of GPR prospection to archaeological sites in Japan. In 14th IEEE International Conference on Ground Penetrating Radar, 2012, pp. 616–619.
11. Kim, J.-H., Yi, M.-J., Son, J.-S., Cho, S.-J. and Park, S.-G., Effective 3D GPR survey and its application to the exploration of old remains. In Proceedings of the IEEE International Geoscience and Remote Sensing Symposium, IGARSS'05, 2005, vol. 1, p. 4.
12. Piro, S. and Goodman, D., Advances in Imaging of Archaeological Structures using GPR. Session 4A5 SC5 High Resolution Imaging with Penetrating Radar Scanners Detect. Small or Low Contrast Objects, 2013, 1377.
13. Novo, A., Lorenzo, H., Rial, F. I. and Solla, M., From pseudo-3D to full-resolution GPR imaging of a complex Roman site. *Near Surf. Geophys.*, 2012, **10**, 11–15.
14. Sternberg, B. K. and McGill, J. W., Archaeology studies in southern Arizona using ground penetrating radar. *J. Appl. Geophys.*, 1995, **33**, 209–225.
15. Leucci, G. and Negri, S., Use of ground penetrating radar to map subsurface archaeological features in an urban area. *J. Archaeol. Sci.*, 2006, **33**, 502–512.
16. Rodrigues, S. I., Porsani, J. L. and DeBlasis, P. A. D., GPR applied to map Jabuticabeira-II coastal sambaqui archaeological site (Brazil). In 13th International Conference on Ground Penetrating Radar, 2010, pp. 1–5.
17. Conyers, L. B., Discovery, mapping and interpretation of buried cultural resources non-invasively with ground-penetrating radar. *J. Geophys. Eng.*, 2011, **8**, S13.
18. Sravanthi, S., Malik, J. N. and Vikrama, B., Ground penetrating radar investigations at Ahichhatra: an attempt to identify buried subsurface structures. In 14th International Conference on Ground Penetrating Radar, 2012, pp. 625–630.
19. Goodman, D., Nishimura, Y. and Rogers, J. D., GPR time slices in archaeological prospection. *Archaeol. Prospect.*, 1995, **2**, 85–90.
20. Annan, A. P., GPR – history, trends, and future developments. *Subsurf. Sens. Technol. Appl.*, 2002, **3**, 253–270.
21. Niltawach, N., Chen, C.-C., Johnson, J. T. and Baertlein, B. A., A numerical study of buried biomass effects on ground-penetrating radar performance. *IEEE Trans. Geosci. Remote Sensing*, 2004, **42**, 1233–1240.
22. Grasmueck, M., Weger, R. and Horstmeyer, H., Full-resolution 3D GPR imaging. *Geophysics*, 2005, **70**, K12–K19.
23. Conyers, L. B., Ground-penetrating radar techniques to discover and map historic graves. *Hist. Archaeol.*, 2006, 64–73.
24. Conyers, L. B., *Interpreting Ground-Penetrating Radar for Archaeology*, Left Coast Press, 2012.
25. Goodman, D. and Piro, S., *GPR Remote Sensing in Archaeology*, Springer, 2013.
26. Bisht, R. S., Excavations at Dholavira. Excavation report to Archaeological Survey of India, 2015.
27. Agrawal, S., George, N. V. and Prashant, A., GPR data analysis of weak signals using modified S-transform. *Geotech. Geol. Eng.*, 2015, **33**(5), 1167–1182.
28. Vaughan, C. J., Ground-penetrating radar surveys used in archaeological investigations. *Geophysics*, 1986, **51**, 595–604.
29. Conyers, L. B., Ground-penetrating radar processing and interpretation techniques for archaeology. *FastTIMES*, 2008, **13**(3), 29–35.
30. Shukla, S. B., Patidar, A. K. and Bhatt, N., Application of GPR in the study of shallow subsurface sedimentary architecture of Modwa spit, Gulf of Kachchh. *J. Earth Syst. Sci.*, 2008, **117**(1), 33–40.
31. Pennock, S. R. *et al.*, Effects of iron pipe corrosion on GPR detection. In 13th IEEE International Conference on Ground Penetrating Radar, 2010.
32. Perez-Gracia, V., Santos-Assuncao, S., Caselles, O., Clapes, J. and Canas, J. A., Study of wood beams in buildings with ground penetrating radar. In 15th International Conference on Ground Penetrating Radar, 2014, pp. 31–35.
33. Naser, M. and Junge, A., Influence of pipe filling, geometry and antenna polarisation on GPR measurements. In 13th International Conference on Ground Penetrating Radar, Lecce, Italy, 2010, pp. 1–6.
34. Bassuk, N., Grabosky, J., Mucciardi, A. and Raffel, G., Ground-penetrating radar accurately locates tree roots in two soil media under pavement, arboriculture & urban forestry. *Arboricult. Urban Forest.*, 2011, **37**(4), 160–166.
35. Schoor, M. V. and Colvin, C., Tree root mapping with ground penetrating radar. In 11th SAGA Biennial Technical Meeting and Exhibition, Swaziland, 2009, pp. 371–374.
36. Malagodi, S., Orlando, L., Piro, S. and Rosso, F., Location of archaeological structures using GPR method: three-dimensional data acquisition and radar signal processing. *Archaeol. Prospect.*, 1996, **3**(1), 13–23.

ACKNOWLEDGEMENTS. We thank the Archaeological Survey of India, Ministry of Culture, Government of India, and Archaeological Sciences Centre, IIT Gandhinagar for support and encouragement. We also thank Dr V. N. Prabhakar and Prof. Michel Danino for help while interpreting the GPR data.

Received 23 September 2015; accepted 14 September 2017

doi: 10.18520/cs/v114/i04/879-887